

Coherent broadband pulse shaping in the mid infrared

Nadia Belabas and Jean-Pierre Likforman

Laboratoire d'Optique Appliquée, École Nationale Supérieure des Techniques Avancées, Ecole Polytechnique–Centre National de la Recherche Scientifique Unité Mixte de Recherche 7639, F-91761 Palaiseau Cedex, France

Lionel Canioni

Centre de Physique Moléculaire Optique et Hertzienne, Université Bordeaux I–Centre National de la Recherche Scientifique Unité Mixte de Recherche 5798, F-33405 Talence Cedex, France

Bruno Bousquet

Laboratoire de Spectrométrie et Optique Laser, Université de Bretagne Occidentale, F-29285 Brest Cedex, France

Manuel Joffre

Laboratoire d'Optique et Biosciences, Institut National de la Santé et de la Recherche Médicale Unité 7645, Ecole Polytechnique, Ecole Nationale Supérieure des Techniques Avancées, F-91128 Palaiseau Cedex, France

Received December 13, 2000

We demonstrate broadband infrared pulse shaping by difference-frequency mixing of two visible phase-locked linearly chirped pulses in GaAs. Control of the temporal profile of the emitted field is achieved through this direct tailoring of the exciting visible intensity. The results are in agreement with a simulation with no adjustable parameter. © 2001 Optical Society of America

OCIS codes: 320.5540, 260.3060, 320.1590.

Sequences of infrared femtosecond laser pulses permit the probing of chemical or biological ultrafast dynamics. If such pulses are carefully tailored, coherent control of vibrational wave-packet evolution can be performed. In particular, schemes have been proposed for control of single-bond molecular excitation or dissociation with an intense ultrashort laser pulse that is appropriately chirped to match molecular anharmonicity.¹ Pulse shaping in the optical domain has been achieved with various techniques,^{2–4} but control over molecular vibrations requires engineering of a broadband field in amplitude and phase in the mid-infrared (5–20- μm) domain.

In their pioneering experiments, Auston and co-workers⁵ put to good use the command of optical pulses to generate far-infrared tunable narrow-band radiation in nonlinear crystals. In those experiments, a quasi-periodic sequence of short pulses of tunable period T , related to the far-infrared emitted frequency, $1/T$, was formed by means of beating between two identical linearly chirped pulses.^{5–7} Such a pulse train can also arise from shaping with a liquid-crystal modulator.⁸ Shaping experiments in the mid-infrared domain were recently reported⁹ in which the emitted field was fully characterized by electro-optic sampling. In those experiments the optical pulse was shaped as described in Ref. 8 and focused on a 500- μm -thick GaSe crystal. Mid-IR pulse generation was then dictated by phase matching, which prevented direct control of the emitted mid-infrared field. Moreover, the emitted field was spectrally limited to the phase-matching bandwidth.

In this Letter we report on the generation in $\langle 1\bar{1}0 \rangle$ GaAs of broadband mid-infrared shaped pulses by op-

tical rectification of a sequence of two phase-locked chirped visible pulses. As in Ref. 5, we rely on optical rectification to shape mid-infrared field transients. We thus achieve direct control of the mid-infrared emitted field, unlike with emission from phase-matched crystals,⁹ in which the relation between the incident and the generated infrared pulses is more intricate.

Assuming that the second-order susceptibility of the emitting material, $\chi^{(2)}(\omega_1, \omega_2)$, is constant over the spectrum of the exciting pulse, the optical rectification part of the nonlinear polarization, $P^{(2)}(t)$, is simply proportional to the exciting intensity, $I_{\text{exc}}(t)$. This polarization in turn radiates an electric field whose propagation depends on the exact experimental conditions. In the case of a plane-wave excitation and a thin nonlinear material, this field can be calculated to be proportional to the first derivative of the induced polarization.¹⁰ After a Fourier transform (FT) to the spectral domain, the field reads as

$$E_{\text{IR}}(\omega) \propto i\omega \times \text{FT}[I_{\text{exc}}(t)]. \quad (1)$$

For an exciting pulse in the 15-fs range, the generated electric field, $E_{\text{IR}}(\omega)$, has frequency components extending to the mid infrared.¹¹ Furthermore, this straightforward relation between the FT of $I_{\text{exc}}(t)$ and the emitted field¹² provides a unique technique for shaping the mid-infrared field. We demonstrate this fact by use of an exciting intensity of variable shape that arises from beating between two linearly chirped visible pulses, $E_1(t)$ and $E_2(t)$, separated by a variable time delay, τ . The intensity of the total exciting field is then

$$I_{\text{exc}}(t) = |\mathcal{E}_1(t) + \mathcal{E}_2(t - \tau)|^2 \\ = |\mathcal{E}_1|^2 + |\mathcal{E}_2|^2 + [\mathcal{E}_1^*(t)\mathcal{E}_2(t - \tau) + \text{c.c.}]. \quad (2)$$

Considering the amount of chirp used in the experiment, we note that the optical rectification of the first two terms results in low-frequency components that are below the spectral range of our mid-infrared detector. In contrast, the cross terms inside brackets in Eq. (2) can result in fast-oscillating beating of frequency $\omega_{\text{IR}}(t)$ that yields mid-infrared radiation after optical rectification, a process that can also be viewed as difference-frequency mixing between the two pulses. The phase of these cross terms is the phase difference between $\mathcal{E}_1(t)$ and $\mathcal{E}_2(t - \tau)$, and so we must stabilize time delay τ during the whole measurement to avoid any phase fluctuation in the emitted field.

If we call φ_1'' and φ_2'' the second derivatives at the center frequency of the spectral phase of pulses 1 and 2, respectively, each pulse can be associated with an instantaneous frequency, $\omega_i(t) \approx \omega_0 + t/\varphi_i''$. The beating frequency is thus $\omega_{\text{IR}}(t) \approx \text{sgn}(\tau\Delta\varphi'') (1/\varphi_1'' - 1/\varphi_2'')t + |\tau|/\varphi_2''$. Two cases can be considered, depending on the value of $\Delta\varphi'' = \varphi_1'' - \varphi_2''$. If $\Delta\varphi'' = 0$, the generated frequency is well defined and is simply equal to τ/φ_2'' ; in this case, tunable narrow-band mid-infrared radiation is generated, similarly to what was reported in Ref. 5. If $\Delta\varphi'' \neq 0$, the generated frequency scans a broader range, and a chirped broadband mid-infrared pulse is then emitted. The value of the second-order derivative of the spectral phase in the infrared, φ_{IR}'' , can be easily deduced from the slope of $\omega_{\text{IR}}(t)$:

$$\frac{1}{\varphi_{\text{IR}}''} = \text{sgn}(\tau\Delta\varphi'') \left(\frac{1}{\varphi_1''} - \frac{1}{\varphi_2''} \right). \quad (3)$$

This result can also be obtained in the frequency domain by means of a stationary phase approximation. Below, we go beyond this simple model and simulate our results directly, using an actual experimental exciting-pulse profile.

The experimental setup is shown in Fig. 1. We use a Ti:sapphire oscillator with a 100-MHz repetition rate that delivers visible pulses of 20-fs duration, with a spectrum stretching over $[0.745\text{--}0.885 \mu\text{m}]$. The spectral phase of the pulses has been characterized with a spectral phase interferometry for direct electric field reconstruction setup¹³ and found to be of the order of 5 fs^2 , which causes negligible temporal broadening of the pulse. $\mathcal{E}_1(t) + \mathcal{E}_2(t - \tau)$ is the output of a phase-locked Mach-Zehnder interferometer. Chirping is achieved by linear dispersion in identical 17.2-mm-thick SF58 glass pieces. A single piece at position (a) yields $\Delta\varphi'' = 0$, and one piece at position (a) and a second at position (b) yield $\varphi_1'' = 2\varphi_2''$, $\Delta\varphi'' \neq 0$.

$I_{\text{exc}}(t)$ can be calculated without any adjustable parameter: The spectra of \mathcal{E}_1 and \mathcal{E}_2 are measured with a spectrometer, which also permits FT spectral interferometry,¹⁴ i.e., very precise measurement of delay τ and the spectral phases and absorption induced by the glass pieces. The phases of \mathcal{E}_1 and \mathcal{E}_2 are locked¹⁵ at

$\pi/2$. The choice of this value influences only the absolute phase of the infrared emitted field.

$\mathcal{E}_1(t) + \mathcal{E}_2(t - \tau)$ is focused on a 100- μm -thick GaAs crystal. The emitted field, \mathcal{E}_{IR} , is then detected by use of diffracting infrared FT spectroscopy.¹⁶ The cross correlation between \mathcal{E}_{IR} and a reference mid-infrared pulse, \mathcal{E}_{REF} , that is nearly single cycle is recorded as a function of time delay T between \mathcal{E}_{IR} and \mathcal{E}_{REF} . Wigner functions computed from the experimental signal, $S(T)$, are plotted in Figs. 2(a) and 2(b) for $\varphi_1'' = 2\varphi_2''$. Comparison of these functions with the Wigner functions of the fast-oscillating cross term of $I_{\text{exc}}(t)$ in Figs. 2(c) and 2(d) illustrates the very direct shaping relation of Eq. (1): Both exhibit comparable chirp, as is confirmed more quantitatively below.

Provided that the detector's spectral response curve $R(\omega)$ is well characterized, Fourier treatment of $S(T)$

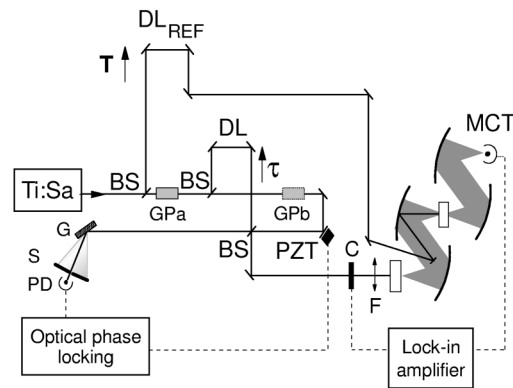


Fig. 1. Experimental layout of pulse-shaped mid-infrared generation. The open rectangles are identical 100- μm -thick $\langle 1\bar{1}0 \rangle$ GaAs sampled. DL's delay lines; BS's, beam splitters; PZT, piezoelectric transducer, C, chopper; F, focalizing optics; MCT, mercury cadmium telluride infrared detector; G, grating; S, slit; PD, photodiode; GPa, GPb glass piece at positions (a) and (b), respectively; Ti:Sa, Ti:sapphire oscillator.

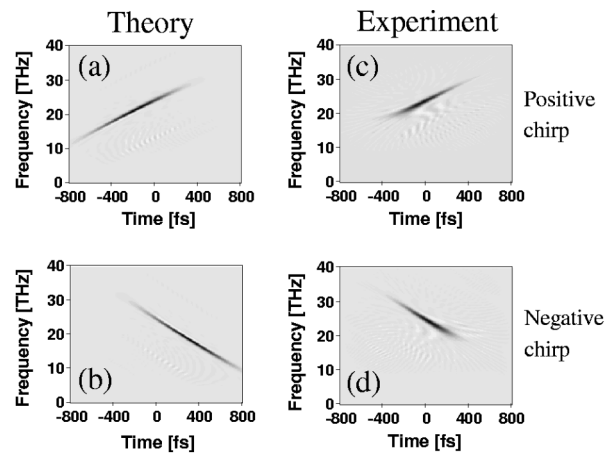


Fig. 2. Wigner functions of (a), (b) the experimental cross-correlation interferograms and (c), (d) the corresponding fast-oscillating term in the calculated visible intensity, $I_{\text{exc}}(t)$. $\varphi_1'' = 2\varphi_2'' = 9220 \text{ fs}^2$ at (a), (c) $\tau = -1 \text{ ps}$ and (b), (d) $\tau = +1$. The discrepancies between experiment and theory (cutoff and broadening) result from the low-frequency cutoff of the detector.

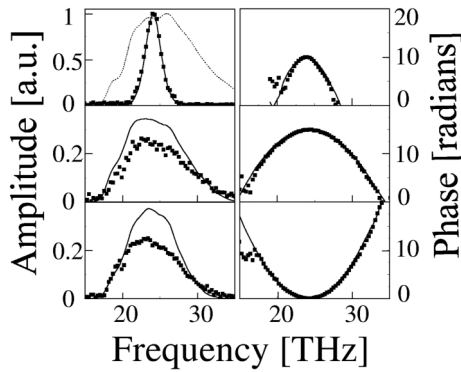


Fig. 3. Experimental and calculated (left) amplitude and (right) phase of the emitted mid-infrared pulse. The squares indicate the experimental points, and the curves are simulations derived from the calculated value of $I_{\text{exc}}(t)$ (see text). Top, $\varphi_1'' = \varphi_2'' = 4610 \text{ fs}^2$ and $\tau = 687 \text{ fs}$; middle, $\varphi_1'' = 2\varphi_2'' = 9220 \text{ fs}^2$ and $\tau = +1 \text{ ps}$; bottom, $\varphi_1'' = 2\varphi_2'' = 9220 \text{ fs}^2$ and $\tau = -1 \text{ ps}$. The additional dotted curve in the top-left-hand plot shows the field amplitude emitted by optical rectification of a single Fourier-limited visible pulse.

gives one access to $\mathcal{E}_{\text{REF}}^*(\omega)\mathcal{E}_{\text{IR}}(\omega)$. In our case, only the spectrum of the reference pulse $|\mathcal{E}_{\text{REF}}(\omega)|^2$ is known. However, the frequency-dependent spectral phase that is accumulated as a result of dispersion through the GaAs generation crystal is measured and found to remain smaller than 0.3 rad within the spectral range of interest. As this value is far smaller than the spectral phase of the measured shaped pulses, the spectral phase of the reference pulse was assumed to be frequency independent. Aside from this assumption, our measurement is sensitive to the complete field \mathcal{E}_{IR} , unlike in the study reported in Ref. 5, in which only the spectral amplitude of the emitted terahertz field was measured.

The amplitude, $A_{\text{IR}}(\omega)$, and the phase, $\varphi_{\text{IR}}(\omega)$, of the FT of $S(T)$ are plotted in Fig. 3 (squares) as $A_{\text{IR}}(\omega)\exp[i\varphi_{\text{IR}}(\omega)] = R(\omega)\mathcal{E}_{\text{REF}}^*(\omega)\mathcal{E}_{\text{IR}}(\omega)$. We apply Eq. (1) and this last expression to the computed value of $I_{\text{exc}}(t)$ to simulate the experimental results.

For $\Delta\varphi'' = 0$, the estimate of the center infrared frequency, $\omega_{\text{IR}} = \tau/\varphi_1''$, given above yields $\omega_{\text{IR}} = 24.1 \text{ THz}$, in excellent agreement with the experiment. As expected, the measured spectrum in Fig. 3 (squares in the top row) is very significantly narrower than the broad amplitude of $R(\omega)|\mathcal{E}_{\text{REF}}(\omega)|^2$ (dotted curve). Furthermore, we tuned this narrow-band radiation from 19.7 to 35.5 THz by varying τ . In the case of $\Delta\varphi'' \neq 0$, Eq. (3) yields $\varphi_{\text{IR}}'' = \varphi_1'' = 2\varphi_2'' = 9220 \text{ fs}^2$, which agrees (to within less than 10%) with the experimental values. Comparison between the experimental data and the simulation shows that the emitted infrared field is very directly linked to the time-dependent optical intensity, $I_{\text{exc}}(t)$, and is thus perfectly controllable. Discrepancies that are especially noticeable

in the amplitude can arise from our assumption of an instantaneous $\chi^{(2)}$ (which is questionable close to the absorption edge) and from the assumed transfer function.¹²

In conclusion, we have demonstrated that optical rectification permits direct broadband shaping in the mid infrared by shaping of visible pulses. In particular, we were able to generate coherent mid-infrared transients of various shapes, including tunable narrow-band radiation and broadband radiation with a controllable amount of second-order dispersion, either positive or negative. These results demonstrate that existing near-infrared pulse-shaping techniques permit the generation of arbitrarily shaped mid-infrared pulses. Amplification of such pulses is the next step toward direct coherent control of molecular vibrations by use of mid-infrared radiation.

We acknowledge fruitful discussions with Paul B. Corkum and support from the National Research Council of Canada–Centre National de la Recherche Scientifique collaborative research project. N. Belabas’s e-mail address is nadia.belabas@polytechnique.org.

References

1. S. Chelbowski, A. D. Bandrauk, and P. B. Corkum, *Phys. Rev. Lett.* **65**, 2355 (1990).
2. A. M. Weiner, D. E. Leaird, J. S. Patel, and J. R. Wullert, *IEEE J. Quantum Electron.* **28**, 908 (1992).
3. Ch. Dorrer, F. Salin, F. Verluise, and J.-P. Huignard, *Opt. Lett.* **23**, 709 (1998).
4. F. Verluise, V. Laude, Z. Cheng, Ch. Spielmann, and P. Tournois, *Opt. Lett.* **25**, 575 (2000).
5. A. S. Weling, B. B. Hu, N. M. Froberg, and D. H. Auston, *Appl. Phys. Lett.* **64**, 137 (1994).
6. G. Veitas and R. Danielus, *J. Opt. Soc. Am. B* **16**, 1561 (1999).
7. A. S. Weling and T. F. Heinz, *J. Opt. Soc. Am. B* **16**, 1455 (1999).
8. Y. Liu, S. G. Park, and A. M. Weiner, *Opt. Lett.* **21**, 1762 (1996).
9. F. Eickemeyer, R. A. Kaindl, M. Woerner, and A. M. Weiner, *Opt. Lett.* **25**, 1472 (2000).
10. A. Bonvalet and M. Joffre, *Femtosecond Laser Pulses* (Springer-Verlag, Berlin, 1998), Chap. X.
11. A. Bonvalet, M. Joffre, J.-L. Martin, and A. Migus, *Appl. Phys. Lett.* **67**, 2907 (1995).
12. For more-accurate shaping or increasing thickness and absorption of the nonlinear material, the $i\omega$ term in Eq. (1) should be replaced with the exact frequency dependence of the transfer function (measured experimentally or calculated with a theory including propagation effects).
13. C. Iaconis and I. A. Walmsley, *IEEE J. Quant. Electron.* **35**, 501 (1999).
14. C. Dorrer, N. Belabas, J.-P. Likforman, and M. Joffre, *J. Opt. Soc. Am. B* **17**, 1795 (2000).
15. L. Canioni, M. Martin, B. Bousquet, and L. Sarger, *Opt. Commun.* **151**, 241 (1998).
16. A. Bonvalet, J. Nagle, V. Berger, A. Migus, J.-L. Martin, and M. Joffre, *Phys. Rev. Lett.* **76**, 4392 (1996).